CONF-8510168--4

THE EFFECT OF POINT DEFECTS ON THE AMORPHIZATION OF METALLIC ALLOYS DURING ION IMPLANTATION*

D. F. PEDRAZA AND L. K. MANSUR
Oak Ridge National Laboratory, Oak Ridge, Tennessee 37831, USA

CONF-8510168--4

DE86 003088

Abstract

A theoretical model of radiation-induced amorphization of ordered intermetallic compounds is developed. The mechanism is ~~taken~~ proposed to be the buildup of lattice defects to very high concentrations, which destabilizes the crystalline structure. Because ~~it is found by calculation~~ that simple point defects do not normally reach such levels during irradiation, a new defect complex ~~is~~ hypothesized containing a vacancy and an interstitial. Crucial properties of the complex are that the interstitial sees a local chemical environment similar to that of an atom in the ordered lattice, that the formation of the complex prevents mutual recombination and that the complex is immobile. The evolution of a disorder based on complexes is not accompanied by ~~any sort of~~ like point defect aggregation. The latter leads to the development of a sink microstructure in alloys that do not become amorphous. For electron irradiation, the complexes form by diffusional encounters. For ion irradiation, complexes are ~~taken to be~~ also formed, ~~in addition,~~ directly in cascades. The possibility of direct amorphization in cascades is also included. Calculations for the compound NiTi show reasonable agreement with measured amorphization kinetics.

---

*Research sponsored by the Division of Materials Sciences, U.S. Department of Energy, under contract DE-AC05-84OR21400 with Martin Marietta Energy Systems, Inc.

1. Introduction

Amorphous metallic alloys are a focus of active research because of both possible technological applications and fundamental scientific aspects. Conventional amorphization procedures start from either the gaseous (e.g., vapor deposition onto cold substrates) or the liquid phase (e.g., splat quenching and melt spinning techniques), both based upon very fast cooling rates. Particle bombardment techniques, on the other hand, start with crystalline solids. It has been suggested that ion irradiation produces conditions far more severe than those that arise on very fast quenching. This is tantamount to asserting that a state of disorder similar to that encountered in the liquid is produced locally by the collision cascades, which then "freeze" at an ultrafast rate [1]. This means that after a certain dose, the entire crystalline target will have experienced displacement cascades and thus become amorphous.

However, not only ion bombardment but also electron irradiation can induce the crystalline to amorphous transition. In this instance, no displacement cascades are produced. Instead, the amorphization phenomenon has to be related to the behavior of the radiation-induced point defects. Comparing the effects produced by each particle type may provide an understanding of the effect of point defects and also of effects due to displacement cascades. We thus aim in the present work to gain some insight into the mechanisms of amorphization in intermetallic compounds. A brief review of published observations is first presented in order to provide a phenomenological background. Next, we discuss the role of point defects, and propose a mechanism of amorphization by

electron irradiation. Finally, the effects of ion bombardment are compared to the previous one in order to single out the effects of collision cascades. Mathematical models are developed for both cases and applied to NiTi.

2. Experimental Background

Ordered intermetallic alloys became a focus of interest because of their potential applications in nuclear reactors. Howe and Rainville [2] investigated the phase stability of Zr_3Al and of Zr_2Al in the temperature range 30–693K. In Zr_3Al they observed the formation of a fairly complex damage configuration accompanied by a gradual decrease of the degree of order and subsequent amorphization with increasing dose. The damage microstructure was suggested ~~as~~ to be due to point defect clusters--no dislocation loops or networks were observed. This result behavior was opposite to that of α (Zr)-solid solution (present in the intermetallic-based samples), which was observed both at high and low temperatures to remain crystalline and to develop a microstructure consisting of small defect clusters, dislocation loops, and dislocation networks. The compound Zr_2Al, ~~also contained in the samples,~~ exhibited a similar propensity to amorphization under ion bombardment. However, this behavior is not observed under electron irradiation, at least at temperatures higher than 130K [3,4]. While Zr_2Al readily becomes amorphous at a low dose, Zr_3Al remains crystalline up to a dose of ~9 dpa [4] (see Table I). Some signs of amorphization were observed at T > 130K by Carpenter and Schulson at a dose of 11 dpa [3].

The stability of different phases of the binary system Ti-Ni has been investigated by several authors [4–14] both under Ni^+ ion and electron bombardments. As in the previous case, ~~it became evident that~~ the propensity to undergo the transition does not depend solely upon the base elements, nor is it unambiguously related to a particular physical property of the compound. Thus, Brimhall et al [5–7] obtained under ions, amorphization of NiTi and $NiTi_2$ after ~0.5 dpa, but not of Ni_3Ti after large doses. Similar behavior was observed in NiTi and Ni_3Ti compounds under electron irradiation [8–10]. Again, some differences were observed between the two types of irradiation in NiTi. While under electrons a transition sequence has been reported [8–11] following the path from martensite → ordered austenite → disordered austenite → amorphous state, this is not the case with ion bombardments where a considerable degree of order remains in the crystalline portion of partly amorphized samples [7,11].

A very marked temperature dependence of the dose necessary to produce complete amorphization was measured by Mori et al. [4,8] in various intermetallics under electron irradiation. ~~Under ions, a~~ temperature dependence was also reported for ion irradiation by Brimhall et al. [7]. The critical temperature at which amorphization is inhibited is apparently higher under ion irradiation.

The amorphization kinetics has been measured in NiTi by Brimhall et al. [7] and my Moine et al. [11]. Although the dose required for rendering the samples amorphous at similar temperatures obtained by the

two groups were nearly the same, the incubation time for the process to commence apparently differed by a factor of 5. The most noticeable difference between the two experiments was the ion energy (400 keV in [11] and 2.5 MeV in [7]).

Some effects of the pre-existing microstructure ~~prior to amorphization~~ have been pointed out by Mori and Fujita [8] who found that the transition in NiTi (under electron irradiation) started in the vicinity of dislocations and grain boundaries. Similarly in Zr_3Al, Carpenter and Schulson [3] allude to possible localized centers where the crystalline to amorphous transition might have occurred, as evidenced for instance by the blurring and subsequent disappearance of pre-existing dislocations after a dose of 11 dpa.

Other intermetallic compounds that were subjected to ion irradiation (see Table I) showed similar characteristics to those pointed out above. Namely, those phases that were not rendered amorphous showed a variety of microstructural changes such as the formation of dense dislocation networks after high doses or even phase transformations to metastable phases, as observed in σ-FeV [6] and Fe-40% Al [12]. On the other hand, no such evolution is apparent in alloys that become amorphous. This suggests that the two groups of metallic alloys differ essentially in the manner in which the radiation-induced point defects are accommodated. This aspect is further analyzed in the next section.

3. Theory

3.1 Mechanisms Leading to Amorphization

Irradiation-induced microstructural changes can be recognized as a path for reducing the excess energy of an open system in a manner compatible with its kinetic constraints. Thus, the formation of voids, dislocation loops, and networks, for instance, originate from like-point defect aggregation. In their subsequent evolution, those extended defects serve as additional sinks for the continuously generated point defects, thus reducing their concentrations and concomitantly the excess energy associated with them. As emphasized in the preceding section, this path is apparently avoided in intermetallic compounds that have a propensity to become amorphous. It may therefore be suggested that those materials are intrinsically resistant to like-point defect aggregation.

It can also be reasoned that it is necessary to have a highly defective lattice in order to destabilize the crystalline structure. Therefore, mutual point defect recombination is inhibited. Indeed, it can be construed from measurements on the crystallization enthalpy of amorphous metallic systems [e.g., ref. [13]) that a defect buildup of ~2% is required to promote amorphization. ~~In this connection~~ we have shown [14], using a rate theory calculation, that a buildup of simple point defects to this level is not possible if at least one of the point defects is mobile and recombination is allowed within 1–3 interatomic distances.

This leads us to introduce the necessity of a distinct defect based upon the Fenkel pair, that may accumulate with increasing dose in a certain temperature range. The simplest such defect that can be visualized is a complex defect containing a vacancy and an interstitial.

Let us next analyze the factors that determine the formation of complexes in some intermetallic compounds. These compounds exhibit long range order at the temperatures of interest. The generation of point defects and their evolution during irradiation perturbs that order. Among the interstitial sites, we may single out those where the chemical nature of the geometric neighbors may allow a given atomic species to create a situation resembling that in the normal ordered lattice. We have proposed [14] that if an interstitial of the appropriate species is generated at or it attains by diffusional migration such a site, it will have a higher tendency of remaining in it if there is a nearby vacancy. The role of the vacancy in the trapping process is that of allowing for partial volume relaxation. The formation of the complex thus constitutes a mechanism for relaxing local stresses while creating a center of short-range order and a focus of topological disorder under irradiation conditions. This is exactly what is necessary for promoting a disordered structure.

It is apparent from this picture that a number of neighboring atoms is involved and hence the complex is an immobile defect. It should also be emphasized that although the crystal around the complex is relaxed, the two point defects maintain their identity as long as the crystalline

structure prevails. These two properties allow us to study the rate of accumulation of complexes and their spatial distribution. In Fig. 1, we illustrate a complex configuration based on a dumbbell interstitial in a bcc lattice.

For electron irradiation this complex would form when the mobile interstitial encounters, by diffusional migration, an immobile vacancy. For ions, however, complexes may form directly in the cascade athermally, in addition to the diffusional process. The probability also exists of amorphization occurring directly as a result of cascade collapse. Both mechanisms may operate in principle concurrently. Two experimental facts indicate that defect formation occurs mainly in the cascade region. One is that amorphization occurs to lower doses under ions than under electron irradiation [11] and the other is that at variance with the electron case, amorphization progresses while the remaining crystal remains ordered [7,11]. This means that the cascade efficiency for producing free point defects is fairly low.

3.2 Amorphization by Electron Irradiation

Both the Frenkel pair creation under electron bombardment and the collision cascades generated by energetic ions are random events. Since these complexes are necessarily immobile defects, their spatial distribution is random as well and can therefore be described by a Poisson distribution. In that description, the critical number of complexes necessary to render a region amorphous and the size of that region must be known.

An analysis of the sensitivity of the theoretical results with respect to the magnitude of those two parameters is done in reference [14].

Let v_0 be defined as an elemental volume containing n_0 atoms where, if the critical number of complexes (m + 1) is obtained, amorphization occurs. Let ζ_i be the volume fraction of elemental volumes v_0 that contains i complexes and $\dot{c}_t$ their average rate of increase, where c_t is the average complex concentration per atom. The following equations then describe the rate of change of ζ_i (i = 1,m),

$$\frac{d\zeta_i}{dt} = n_0 \dot{c}_t \zeta_{i-1} - n_0 \dot{c}_t \zeta_i \tag{1}$$

and for the fraction containing no complexes,

$$\frac{d\zeta_0}{dt} = - n_0 \dot{c}_t \zeta_0 \tag{2}$$

Except for the volume change that accompanies the transition, the conservation of atoms determines that

$$\frac{d\zeta_a}{dt} = - \sum_{i=o}^{m} \frac{d\zeta_i}{dt} = n_0 \dot{c}_t \zeta_m \tag{3}$$

where ζ_a is the amorphous fraction at time t. The integrals that satisfy the set of Eqs. (1) and (2) are

$$\zeta_i = \exp(-n_0 c_t) \frac{(n_0 c_t)^i}{i!} \tag{4}$$

for i = o, m, which represent a Poisson distribution. Hence the amorphous fraction is given by

$$\zeta_a = 1 - \exp(-n_0 c_t) \sum_{i=1}^{m} \frac{(n_0 c_t)^i}{i!} \tag{5}$$

where the average concentration of complexes is c_t.

In order to calculate the kinetics of amorphization, it is necessary to evaluate the magnitude of c_t as a function of time. We shall assume that the interstitial diffusivity is sufficiently high as to control all the relevant processes that determine the buildup of defects under irradiation, while vacancies remain essentially immobile.

As described above, a vacancy/interstitial complex forms by random approach of a self-interstitial to a vacancy so that the interstitial becomes trapped in a favorable interstice with the vacancy being within a convenient interaction distance. The complex may be destroyed by thermal release of the interstitial or by recombination of the vacancy with another self-interstitial. Also, it is removed from the complex population when it contributes to the amorphous fraction. In a binary alloy the number of different interstitial types that exist depend on the self-interstitial configuration. If it is single, there are two self-interstitials; if it is a dumbbell, there are three types. The two cases have been treated in detail in ref. [14] and we shall examine here just the dumbbell case. Let c_{t_j} (j = 1, 2, 3) denote the concentration of complexes where j identifies the component self-interstitial whose concentration is c_j. Then the rate of change of the complex concentration is given by

$$-\frac{dc_{tj}}{dt} = \alpha_j c_j c_v - \beta_j c_{tj} \exp - \left(\frac{E_{Bj}}{kT}\right) - (\gamma_1 c_1 + \gamma_2 c_2 + \gamma_3 c_3) c_{tj} - \frac{c_{tj}}{c_t} \frac{(m+1)}{n_0} \frac{d\zeta_a}{dt} \qquad (6)$$

where c_v is the atomic fraction of vacancies and c_t the total complex concentration, $c_t = c_{t_1} + c_{t_2} + c_{t_3}$. The first term in Eq. (6) is the rate of complex formation. The rate coefficient α_j depends upon the degree of order [14]. The second term accounts for the rate of thermal decomposition, where E_{Bj} is the binding energy of the complex. The third term yields the rate of recombination of the vacancy that is in the complex with another interstitial (indirect recombination). The last term is the rate of removal of complexes as they become part of the amorphous fraction [cf. Eq. (3)].

The rate of change of the vacancy concentration is given by

$$\frac{dc_v}{dt} = G - (R+\alpha) c_i c_v + \sum_{j=1}^{3} \beta' c_{tj} \exp\left(-\frac{E_{Bj}}{kT}\right) \qquad (7)$$

Here G is the generation rate of free vacancies, R is a weighted rate of direct recombination, and α is a weighted rate of complex formation,

$$(R+\alpha) c_i = \sum_{j=1}^{3} (R_j + \alpha_j) c_j \qquad (8)$$

and the last term accounts for the thermal release of free vacancies. β_j' may be different from β_j because there is a probability that the

decomposition of the complex results in the direct recombination of the two constituting defects. Finally, the time evolution of the self-interstitial populations is given by

$$\frac{dc_j}{dt} = G_j - (R_j + \alpha_j)\, c_v - k_{is}^2\, D_i\, c_j + \beta_j'\, c_{tj} \exp\left(-\frac{E_{Bj}}{kT}\right) \sum_{k\neq j} (\gamma_k\, c_k\, c_{tj} - \gamma_j\, c_j\, c_{tk}) \qquad (9)$$

G_j is the generation rate of free interstitials of j-type ($G = \sum_{k=1}^{3} G_j$). The second term in Eq. (9) is the rate of loss by direct recombination and by complex formation, the third is the rate of interstitial annihilation at sinks (e.g., dislocations, free surfaces, grain boundaries), the fourth is the rate of thermal release of interstitials (that does not lead to recombination of the pair). The last term expresses the rate of release of an interstitial of class j by indirect recombination with the other interstitial classes, minus the rate of removal of a j-interstitial because of its (indirect) recombination with a vacancy from complex of type k≠j. The simultaneous solution of Eqs. (6), (7), and (9) yields c_t as a function of dose and then the amorphous fraction can be obtained with Eq. (5).

The different elemental processes that have been incorporated into the rate equations are characterized by appropriate rate coefficients. These coefficients are determined by geometric constraints and by the complex configuration. We shall adopt, as an example, the configuration depicted in Fig. 1 where the condition is that the dumbbell be separated

from the vacancy by three diffusional jumps. The pertinent rate coefficients [14] are shown in Table II, for a bcc (B2 type) lattice.

We have applied this model to the case of equiatomic NiTi. Available data for metallic systems (e.g., ref. [15]) indicate that a local buildup of defects to about two percent, the defects having an energy of ~3-4 eV, can account for the measured enthalpy. We have assumed $n_0 = 400$ and $m = 7$. Figure 2 illustrates the variation of ζ versus dose at a given temperature for the set of parameters shown in Table III. Figure 3 shows the dose limits within which 80% and 97% amorphization of an irradiated sample are predicted in NiTi as a function of temperature, together with the experimental data of Mori and Fujita [8].

3.3 Amorphization by Ion Irradiation

As discussed in Section 3.1, possible effects associated with the displacement cascades are direct amorphization or direct (rather than by diffusional encounters) production of complexes. The latter may take place partly at the expense of in-cascade recombination. It may be suggested, therefore, that the complex production rate could be much larger than under electron irradiation. Furthermore, due to the cascade geometry, more complex defect configurtions than the one already proposed might form. We shall account for other possible stable complex configurations by assuming the formation of clusters of the simpler complex. Let s denote the number of complexes in the largest cluster and $c_t(i)$ the concentration of clusters containing i complexes. (For

simplicity, we shall not differentiate here between different self-interstitial kinds forming the complex.) Let us again denote by ζ_i ($i = 0, m$) the volume fraction of regions of n_0 atoms that contain i complexes. Then, the rate of change of those fractions can be described by the following equations

$$\frac{d\zeta_0}{dt} = - n_0 \sum_{r=1}^{s} \dot{c}_t(r)\ \zeta_0 - K\varepsilon_a\ \zeta_0 \qquad (10)$$

and, for $\ell = 1, m$

$$\frac{d\zeta_\ell}{dt} = - n_0 \sum_{r=1}^{s} \dot{c}_t(r)\ \zeta_\ell + n_0 \sum_{r=1}^{\ell/s'} c_t(r)\ \zeta_{\ell-r} - K\varepsilon_a\ \zeta_\ell \qquad (11)$$

where $\sum'$ has to be carried up to the smallest value, ℓ or s. The last term in Eqs. (10) and (11) account for direct amorphization in the displacement cascade, with a certain efficiency ε_a, relative to the displacement rate, K. The first term yields the rate of decrease of ζ_i owing to complex formation in the regions already containing i complexes, while the middle term in Eq. (11) yields the rate of increase of ζ_ℓ due to complex formation totaling ℓ, in regions contaning less than ℓ complexes. The solutions of Eqs. (10) and (11) are, for $\ell = o, m$

$$\zeta_\ell = \exp\ (- K\varepsilon_a t)\ \exp\ (-n_0 \sum_{r=1}^{s} c_t(r) \times$$

$$\sum_{m_\ell} \prod_{r=1}^{s} \frac{(n_0 c_t(r)^{j_r(m_\ell)}}{[j_r(m_\ell)]!} \qquad (12)$$

where

$$\sum_{r=1}^{s} r\, j_r(m_\ell) = \ell$$

Some examples of this algebraically involved solution are given in the Appendix. The amorphous fraction can be calculated by substituting equations (12) for ζ_ℓ into equation (5), when no shrinkage of amorphous regions can occur.

As in the case of the previous section, we shall assume that vacancies remain essentially immobile in the temperature range of interest. A rate theory approach is used for calculating the buildup of complexes and complex clusters. For ℓ=2, s, we write

$$\frac{dc_t(\ell)}{dt} = K\varepsilon_\ell + \frac{c_t(\ell+1)}{\tau_{\ell+1}} - \frac{c_t(\ell)}{\tau_\ell} - \frac{1}{\tau_{a\ell}} \tag{13}$$

where

$$\tau_\ell^{-1} = \beta_\ell \exp\left(-\frac{E_{B\ell}}{kT}\right) + \gamma_\ell c_i \tag{14}$$

is the rate coefficient for the destruction of one complex in the cluster of size ℓ by either thermal decomposition or recombination of the constituent vacancy with a free interstitial. Both processes produce a cluster of size ℓ-1. The last term in (13) accounts for cluster removal from the distribution owing to amorphization and is given by

$$\tau_{a\ell}^{-1} = \frac{m+1}{n_o} \frac{c_t(\ell)}{s} \frac{d_{\zeta a}}{dt} \sum_{r=1} rc_r \qquad (15)$$

For the cluster of size s,

$$\frac{dc_t(s)}{dt} = K\varepsilon_s - \frac{c_t(s)}{\tau_s} - \frac{1}{\tau_{as}} \qquad (16)$$

and for single complexes,

$$\frac{c_t(1)}{dt} = K\varepsilon_1 + \alpha c_i c_v + \frac{c_t(2)}{\tau_2} - \frac{c_t(1)}{\tau_1} - \frac{1}{\tau_{a1}} \qquad (17)$$

For equations (16) and (17) the coefficients τ_1, τ_2, τ_s, τ_{a1}, τ_{as} are given by expressions similar to equations (14) and (15). The possibility of complex formation by random encounter of a vacancy and an interstitial in the matrix has been included in equation (17). The rate equations for vacancies and interstitials are, respectively

$$\frac{dc_v}{dt} = G - (R+\alpha)c_i c_v + \sum_{\ell=1}^{s} \beta_\ell' c_t(\ell) \exp\left(-\frac{E_{B\ell}}{kT}\right) \qquad (18)$$

and

$$\frac{dc_i}{dt} = G - (R+\alpha)c_i c_v - k_{is}^2 D_i c_i + \sum_{\ell=1}^{s} \beta_\ell' c_t(\ell) \exp\left(-\frac{E_{B\ell}}{kT}\right) \qquad (19)$$

where the point defect production rate is given by

$$G = K \left(1 - \sum_{r=1}^{s} r\varepsilon_r - n\right) \tag{20}$$

where nK accounts for in-cascade recombination of Frenkel pairs.

We have applied the present model to the case of ion induced amorphization in NiTi. Two cases were analyzed, viz., s = 1 and s = 2. For both cases we assumed that no direct amorphization takes place in the cascade event, i.e., $\varepsilon_a = 0$. Figure 4 shows the variation of ζ_a vs dose for the set of parameters given in Table IV. It can be noticed, by comparison with Figure 2 that the amorphization kinetics is faster and that there is a temperature shift, relative to the case of electrons, towards higher temperatures. As the temperature is increased, it can be seen that the kinetics becomes progressively slower. At higher temperatures (not shown) the amorphous fraction becomes virtually zero. This is not the case for s = 2, as can be seen in Figure 5. There it can be noticed that, at around the dose where complete amorphization occurs at the lower temperatures (T~300 K), ζ_a tends to a saturation value that decreases with increasing temperature. This would yield either a crystalline matrix with a dispersion of amorphous regions or the other way around.

Figure 6 shows the amorphization kinetics assuming s = 1 and s = 2, when the total production rate of complexes has been assumed to be equal, i.e.,

$$\varepsilon_1(s = 1) = \varepsilon_1(s = 2) + \varepsilon_2(s = 2)$$

and the values of the other parameters are given in Table III. A slightly faster growth of ζ_a is obtained when s = 2, although the total doses for ζ_a = 1 tend to a common value. The results of the experiments by Brimhall et al. [7] and Moine et al. [11] have been included in the Figure. The theoretical curves are shown to fall between the two sets of data and attain virtually complete amorphization in coincidence with the experimental results.

6. Discussion

Based on an analysis of experimental observations, we have reasoned that amorphization is an alternative evolution path to that of developing an irradiation-induced defective lattice. Since the latter is based upon like-point defect aggregation, we have also reasoned that this aggregation must be resisted in compounds that become amorphous. We also concluded that a recombination of Frenkel pairs must be limited in order to provide high enough densities to destabilize the crystalline lattice. A vacancy/interstitial complex was proposed as the simplest complex that could retain both point defects in the lattice. Such a complex and its region of influence exhibit two features that are most likely to promote a transition to the amorphous state. These are the existence of a state of localized topological disorder and a chemical short range order.

We have applied our theory to the case of electron induced amorphization in NiTi and showed that the temperature dependence of the dose required for complete amorphization could be well explained. A more thorough discussion of this problem is carried out elsewhere [14].

For ion bombardment, when amorphization does not occur in a single cascade event, we have reasoned that the complex buildup should be strongly enhanced. We therefore introduced the idea of direct production of complexes in a cascade, in addition to the production of complexes by a diffusional process as for electron irradiation. Then, ions may be much more efficient in inducing amorphization than electrons. The greater efficiency of ions in producing amorphization is supported by experimental observations. For instance, some compounds that are easily rendered amorphous under ion bombardment, e.g., Zr_3Al, FeTi, are resistant under electron irradiation.

We have assumed in both cases that one defect at least (the vacancy in our hypothesis), should remain essentially immobile at the temperatures where amorphization takes place. This should clearly be the case for electron irradiation since complex formation depends on the vacancy as well as on the interstitial content in the material. As can be easily shown [14], only a mobility sufficiently high to allow both defects to limit the life time of the complex by recombination with the corresponding anti-defect, would prevent any substantial buildup. In the case of ions the mobility of both point defects would have also the effect of limiting the life time of a complex. Nevertheless, the formation of amorphous regions might still occur because of the high efficiency of complex production in the cascade.

An important point should be highlighted in this connection. In other studies comparing microstructural damage by ions and electrons where no

amorphous transition occurs, it has been generally found that electrons are more effective per unit displacement in producing microstructural defects such as dislocation loops and cavities. The opposite seems to be the case when amorphization takes place, as ions seem to be more effective than electrons. This can be interpreted to support a very high efficiency for direct complex formation in cascades.

At temperatures where both point defects may have sufficient mobility as to annihilate at sinks, amorphization may still occur by ion bombardment. Shrinkage of amorphized regions could then occur by vacancy/interstitial annihilation at the amorphous-crystal interface. This has been observed for instance in silicon [16,17] partly amorphized with ions and subsequently irradiated with electrons. This phenomenon lead Nelson to formulate a rate theory model of shrinkage of "disordered" regions formed in the displacement cascade region [18].

Our analysis of complex formation under ion bombardment is only preliminary. The possibility of complex entities needing a description distinct from that of the simpler unit that applies in the case of electrons, is only suggested by the geometry of the cascade. This aspect, certainly, needs further study, in particular with reference to the energy of incident ions and the resulting PKA spectrum.

References

[1] W.A. Grant, J. Vac. Sci. Technol. 15 (1978) 1644.

[2] L.M. Howe and M.H. Rainville, J. Nucl. Mater. 68 (1977) 215; Rad. Eff. 48 (1980) 151.

[3] G.J.C. Carpenter and E.M. Schulson, J. Nucl. Mater. 73 (1978) 180.

[4] H. Mori, H. Fujita, M. Tendo, and M. Fujita, Scripta Met. 18 (1984) 783.

[5] J.L. Brimhall, H.E. Kissinger, and L.A. Charlot, Metastable Materials Formation by Ion Implantation, eds., S.T. Picraux and W.J. Choyke (North Holland, New York, 1982) p. 235.

[6] J.L. Brimhall, H.E. Kissinger, and L.A. Charlot, Rad. Eff. 77 (1983) 273.

[7] J.L. Brimhall, H.E. Kissinger, and A.R. Pelton, Ion Implantation and Ion Beam Procesing of Materals, eds., G.K. Husler, O.W. Holland, C.R. Clayton, and C.W. White (North Holland, New York, 1984) p. 63.

[8] H. Mori and H. Fujita, Jpn. J. Appl. Phys. 21 (1982) L404.

[9] H. Mori, H. Fujita, and M. Fujita, Jpn. J. Appl. Phys. 22 (1983) L94.

[10] A.R. Pelton, Proc. Seventh International Conf. on High Voltage Electron Microscopy, LBL-16031, UC-25, CONF-830819 (Berkeley, CA 1983) p. 245.

[11] P. Moine, J.P. Rivière, M.O. Rouault, J. Chaumont, A. Pelton and R. Sinclair, to be published.

[12] J.P. Rivière, M.O. Rovault, M. Schack, and J. Chaumont, Rad. Eff. 79 (1983) 275.

[13] M.L. Swanson, J.R. Parson, and C.W. Hoelke, Rad. Eff. 9 (1971) 249.

[14] D.F. Pedraza, Mechanisms of the Electron Irradiation Induced Amorphous Transition in Intermetallic Compounds, to be published.

[15] A.F. Marshall, Y.S. Lee, and D.A. Stevenson, Acta Metall. 31 (1983) 1225.

[16] R.S. Nelson, Proc. Int. Conf. Radiation Damage in Semiconductors (Reading, 1972) p. 140.

[17] J. Washburn, C.S. Murty, D. Sadana, P. Byrne, R. Gronski, N. Cheung, and R. Kilaas, Nucl. Instr. and Meth. 209/210 (1983) 345.

[18] R.S. Nelson, Rad. Eff. 32 (1977) 19.

APPENDIX

Example that illustrates the application of Equation (12):

Let $s=3$ and $\ell=5$

then,

$$\sum_{r=1}^{s} r j_r(m_\ell) = j_1(m_5) + 2j_2(m_5) + 3j_3(m_5) = 5 \qquad \text{(A.1)}$$

Only the following combinations satisfy Equation (A.1):

$m_5 = 1;$	$j_1 = 5;$	$j_2 = 0;$	$j_3 = 0$
$m_5 = 2;$	$j_1 = 3;$	$j_2 = 1;$	$j_3 = 0$
$m_5 = 3;$	$j_1 = 2;$	$j_2 = 0;$	$j_3 = 1$
$m_5 = 4;$	$j_1 = 1;$	$j_2 = 2;$	$j_3 = 0$
$m_5 = 5;$	$j_1 = 0;$	$j_2 = 1;$	$j_3 = 1$

This gives

$$\sum_{m_5} \prod_{r=1}^{3} \frac{(n_0 c_t(r))^{j_r(m_5)}}{[j_r(m_5)]!} = \frac{(n_0 c_t(1))^5}{5!} + \frac{(n_0 c_t(1))^3 (n_0 c_t(2))}{3!}$$

$$+ \frac{(n_0 c_t(1))^2 (n_0 c_t(3))}{2!} + \frac{(n_0 c_t(1)) (n_0 c_t(2))^2}{2!}$$

$$+ (n_0 c_t(2)) (n_0 c_t(3))$$

TABLE I

Crystal Stability Under Irradiation of Intermetallic Compounds

Compound	Crystal Structure	Amphorization Induced by Electron Irradiation	Test Temperature (K)	Reference	Amphorization[a] Induced by Ion Bombardment	Reference
NiAl	B2	No	160	4	No	5,6
Ni_3Al	$L1_2$	No	160	4	No	5,6
$NiAl_3$	DO_{20}				Yes	6
CoTi	B2	No	160	4		
Co_2Ti	C15	Yes	160	4		
Cr_2Ti	C15	No	160	4		
CuTi	B11	(Yes),(No)	(95-170),(186)	4		
Cu_3Ti_2	tetr	Yes	160	4		
Cu_4Ti	ortho	No	160	4		
FeTi	B2	No	160	4	Yes	5,6
Fe_2Ti	C14	Yes	160	4	Yes	6
Mn_2Ti	C14	Yes	160	4		
		(Yes),(No)	(50-230),(>273)	4,8,9	Yes	(5-11)
		(90,RT)	(Yes;No)[d]	10		
$NiTi_2$	$E9_3$				Yes	5,6
Ni_3Ti	DO_{24}	RT	No	10	No	6
MoNi	tetr	Yes	160	4	Yes	6
Nb_7Ni_6	$D8_5$	Yes	160	4		
Zr_2Ni	C16	Yes	160	4		
CuZn	B2	No	160	4		
CuZr	unknown	Yes	160	4		
$Cu_{10}Zr_7$	ortho	Yes	160	4		
Zr_2Al	C16	Yes	160	4	Yes[c]	2
Zr_3Al	$L1_2$	incomplete	>130	3	Yes[c]	2
		No	160	4		
Re_3Ta	A12				Yes	5,6
Fe-V-σ	$D8_b$				No	6

a The test temperature is room temperature
b Also at 900 K
c Experiments conducted between 30 and 850 K
d Vapor deposited and crystallized sample

TABLE II

Rate Coefficients Describing the Elementary Processes Undertaken by Vacancies and Self-Interstitials (Dumbbell Configuration)

— Complex Formation (One Possible Configuration):

$$\alpha_{Ni} = 10.40 \frac{D_i}{b^2}$$

— Direct Recombination (Second Nearest Neighbors)

$$R = 26.5 \frac{D_i}{b^2}$$

— Indirect Recombination

$$\gamma = 26.5 \phi \exp \frac{D_i}{b_2} \left(- \frac{\Delta E}{kT}\right)$$

— Thermal Decomposition

$$\beta = 3 \frac{D_i}{b^2}$$

— Thermal Decomposition Not Leading to Direct Recombination

$$\beta' = 2.5 \frac{D_i}{b^2}$$

TABLE III

Physical Parameters Used for Calculating the Rate of Amorphization of NiTi

$D_i = 10^{-6} \times \exp(-\frac{0.29\ eV}{kT})\ m/s^2$

$k_{is} = 4.15 \times 10^6\ m^{-1}$ (for electrons)

$k_{is} = 3.10 \times 10^6\ m^{-1}$ (for ions, s = 1)

$k_{is} = 5.28 \times 10^6\ m^{-1}$ (for ions, s = 2)

$E_B = 1.00$ eV

$\Delta E = 0.15$ eV

$C_t^c = 2\%$

$n_o = 400$ atoms

$\phi = 0.53$

$\eta = 0.20$

$E = 0.60$ (s = 1)

For s = 2:

$E_1 = 0.10$

$E_2 = 0.25$

$\beta_2/\beta_1 = 1$

$\Delta E_{B_2}/\Delta E_{B_1} = 1.5$

$\gamma_2/\gamma_1 = 1$

ORNL-DWG 85C-16131

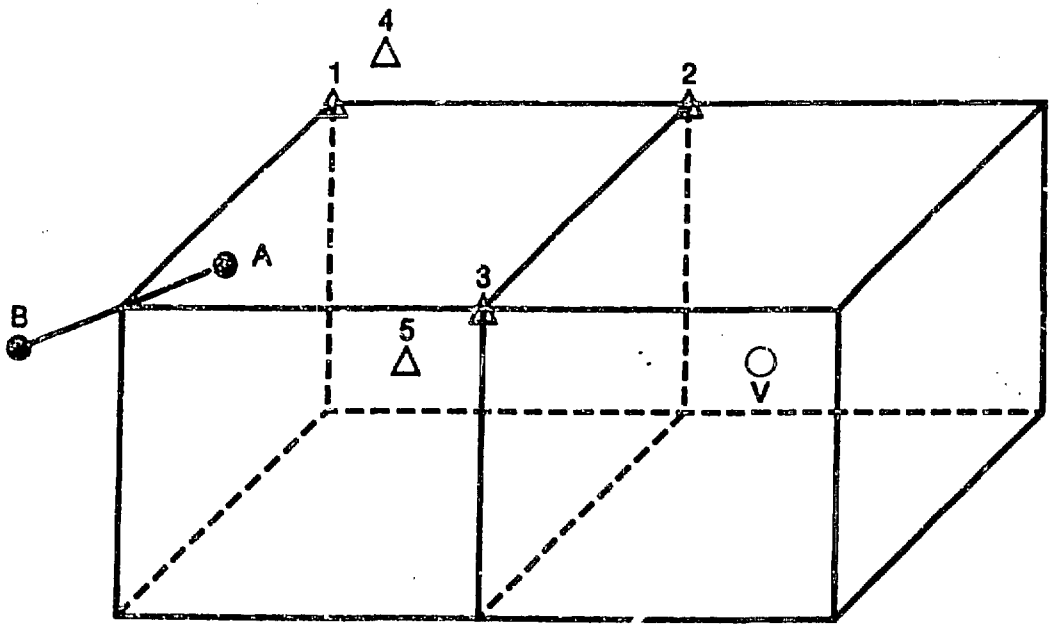

ORNL-DWG 65C-16129

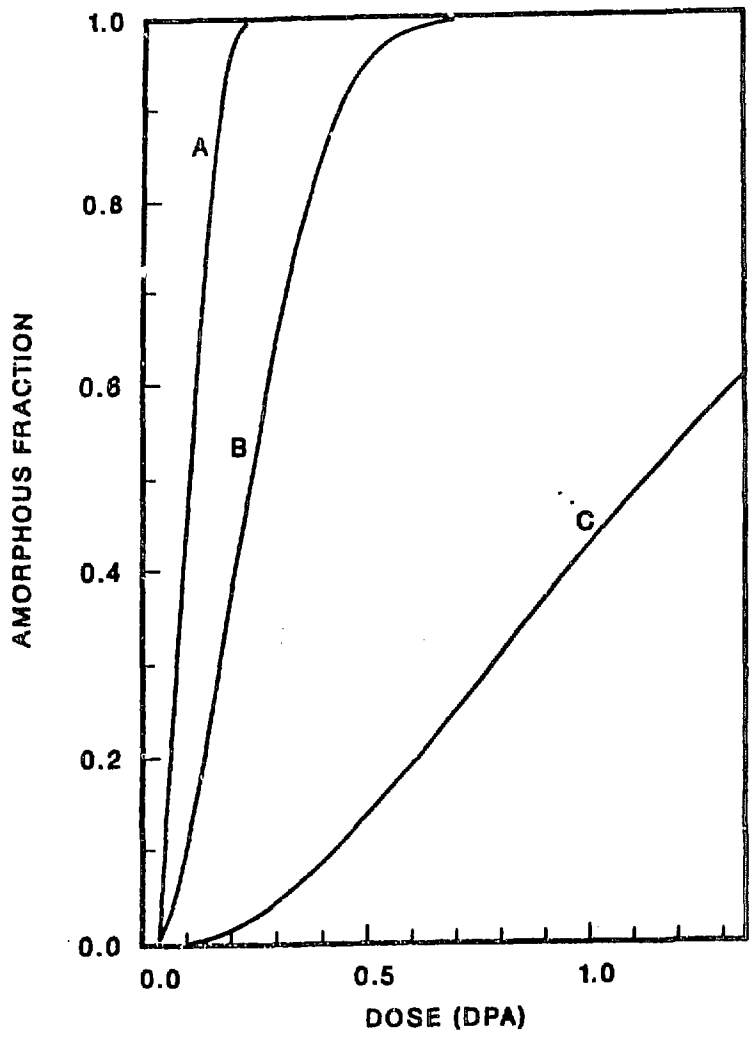

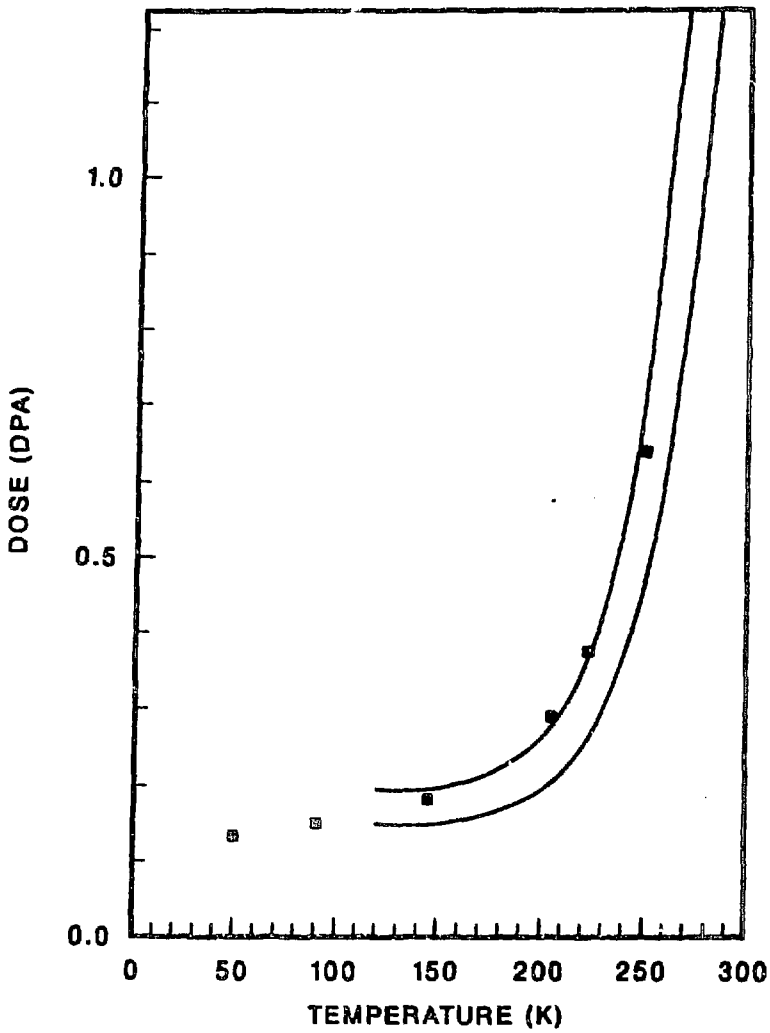
DOSE (DPA)
1.0
0.5
0.0
0
50
100
150
200
250
300
TEMPERATURE (K)

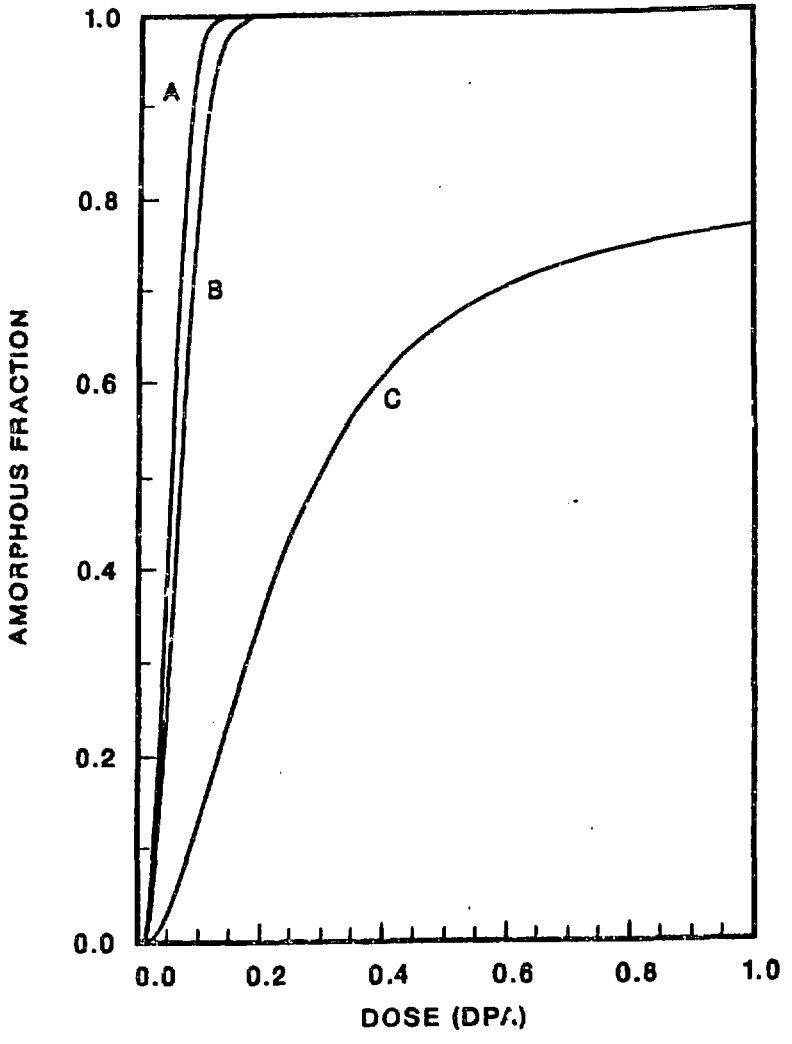
AMORPHOUS FRACTION
1.0
0.8
0.6
0.4
0.2
0.0
A
B
C
0.0
0.2
0.4
0.6
0.8
1.0
DOSE (DPA)

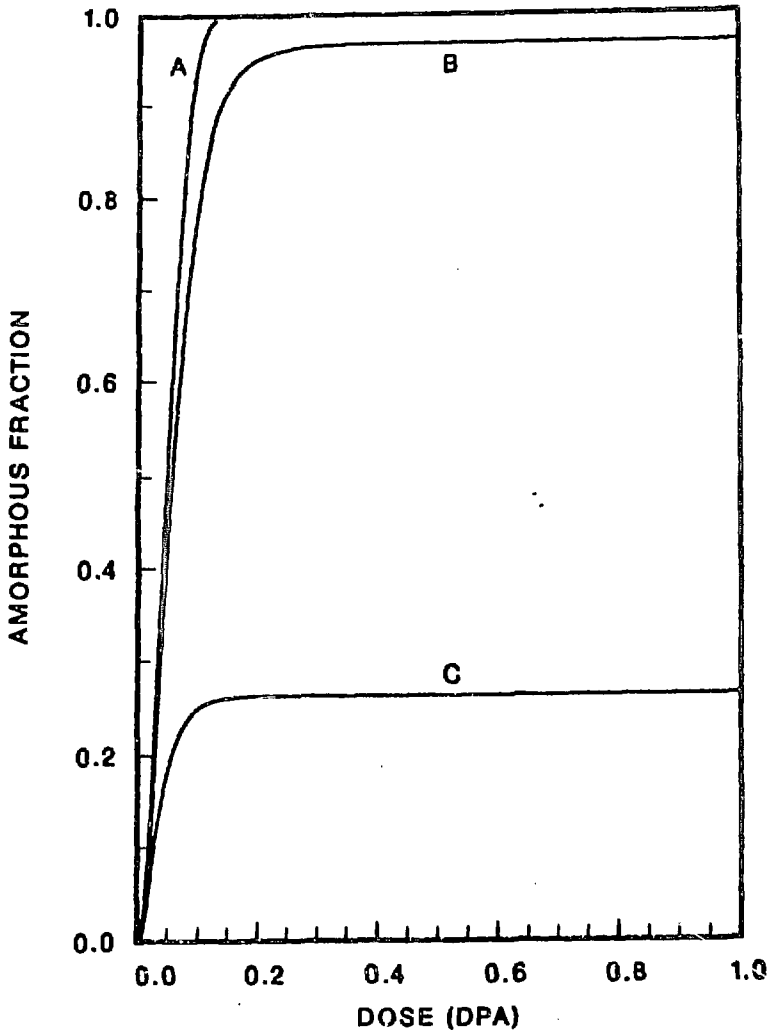
1.0
0.8
0.6
0.4
0.2
0.0
AMORPHOUS FRACTION
A
B
C
0.0
0.2
0.4
0.6
0.8
1.0
DOSE (DPA)

ORNL-DWG 85C-16125

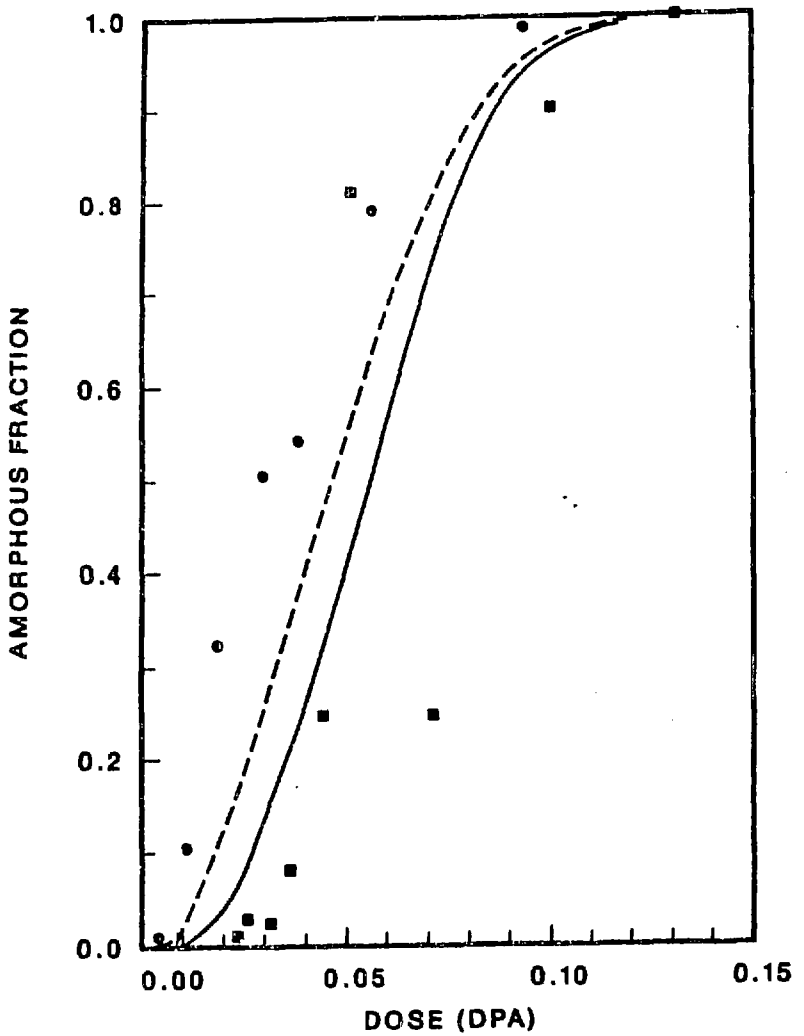

FIGURE CAPTIONS

Figure 1. Complex configuration in a BCC lattice. At least four of the numbered atoms must be of species B for the complex to form. Complex decomposition can occur if the dumbbell jumps out of the indicated site. If it jumps into sites 4 or 5, direct recombination will follow.

Figure 2. Amorphous fraction vs electron dose at various temperatures, A: 150 K, B: 240 K, C: 300 K. The r values of the physical parameters are given in Table II.

Figure 3. Dose required for obtaining a given amorphous fraction under electron irradiation, as a function of temperature. Lower curve, ζ = 80%. Upper curve, ζ = 97%. Stars show experimental data by Mori and Fujita [8].

Figure 4. Amorphous fraction vs ion dose at three different temperatures. A: 300 K, B: 330 K and C: 395 K. Simple complex configuration (s = 1). (The values of the parameters are given in Table III.)

Figure 5. Amorphous fraction vs ion dose at three different temperatures. A: 300 K, B: 390 K and C: 410 K. Single complexes and two-complex clusters (s = 2). (The values of the parameters are tiven in Table III.)

Figure 6. Amorphous fraction vs ion dose at 300 K. Full line: simple complex configuration (s = 1). Dotted line: Two complex clusters and single complexes (s = 2). ▣ Experimental data by Brimhall et al. [7]; ⊙: Experimental data by Moine et al. [11].

DISCLAIMER